Modelling phage-bacteria interactions driving predation and horizontal gene transfer

Jorge A. Moura de Sousa[1,2,*], Ahlam Alsaadi[3], Jakob Haaber[3], Hanne Ingmer[3], Eduardo P.C. Rocha[1,2]

[1]Microbial Evolutionary Genomics, Institut Pasteur, 28, rue Dr Roux, Paris, 75015, France.
[2]CNRS, UMR3525, 28, rue Dr Roux, Paris, 75015, France.

[3]Department of Veterinary and Animal Sciences, University of Copenhagen, Frederiksberg, Denmark

* corresponding author: jorge-andre.sousa@pasteur.fr

SHORT TITLE: eVIVALDI: eco-evolutionary dynamics of phage-bacteria

Keywords: individual based modelling; predation; phage therapy; transduction; antibiotic resistance.

ABSTRACT

Bacteriophages shape microbial communities by predating on them and by accelerating their adaptation through horizontal gene transfer. The former is the basis of phage therapy, whereas the latter drives the evolution of numerous bacterial pathogens. We present a novel computational approach (eVIVALDI – eco-**eV**olutionary m**I**crobial indi**V**idu**AL**-base**D** s**I**mulations) to study phage-bacteria ecological interactions that integrates a large number of processes, including population dynamics, environmental structure, genome evolution, and phage-mediated horizontal transfer. We validate and illustrate the relevance of the model by focusing on three specific questions: the ecological interactions between bacteria and virulent phage during phage and antibiotic therapy, the role of prophages as competitive weapons, and how autotransduction facilitates bacterial acquisition of antibiotic resistance genes upon lysis of antibiotic resistant competitors. Our model recapitulates experimental and theoretical observations and provides novel insights. In particular, we find that environmental structure has a strong effect on community dynamics and evolutionary outcomes in all three case studies. Strong environmental structure, relative to well-mixed environments and especially if antibiotics are heterogeneously distributed, enhances the rate of acquisition of resistance to both phages and antibiotics, and leads to more accurate predictions of the dynamics of lysogen invasion in the gastrointestinal tract. We predicted the co-existence of invaders and resident lysogens in autotransduction under a range of parameters, and validated this key prediction experimentally. By linking ecological and evolutionary dynamics, our modelling approach sheds light on the factors that influence the dynamics of phage-bacteria interactions. It can also be expanded to put forward novel hypotheses, facilitating the design of phage therapy treatments and the assessment of the role of phages in the spread of antibiotic resistance.

AUTHOR SUMMARY

In the face of a growing threat of antibiotic resistant bacteria, bacteriophages have re-emerged as a potential alternative to clinical treatments of infections, as they are efficient bacterial predators. However, bacteriophages can also promote, through a mechanism called transduction, the dissemination of adaptive traits between bacteria, including antibiotic resistance genes. Importantly, these two types of interactions (predation and transduction) can co-occur, which creates difficulties in predicting their outcome. We have developed eVIVALDI (eco-**eV**olutionary m**I**crobial indi**V**idu**AL**-base**D** s**I**mulations), a computational model that allows the simulation of microbial communities with a focus on the mechanisms involved in phage-bacteria interactions, across time and in different types of environments. eVIVALDI can be used to understand the conditions where phages are more likely to be successfully used to eliminate bacteria or, in the other hand, the conditions where they increase the probability of dissemination of adaptive traits. Our research highlights the importance of considering the diverse ways that phage and bacteria interact, and the relevant ecological conditions where these interactions take place, to understand how bacteriophages shape microbial communities and how they can be used as a clinical tool.

Introduction

Microbial organisms are pervasive across all natural environments, including the human body. Their adaptation and organization in communities may lead to disease [1], drive host evolution [2], and produce major changes in ecosystems [3,4]. Ecological interactions in microbial communities influence, and are influenced by, the rapid pace with which microbes acquire adaptive changes [5,6]. A striking example is the relationship between bacteria and bacteriophages (from here on referred to as phages), because the latter predate on the former whilst also driving their adaptation [4]. Phages are the most abundant entities in nature [7,8] and very efficient bacterial predators; it has been estimated that they promote the turnover of ~20% of bacterial mass every single day in certain environments [9,10]. In the context of widespread antibiotic resistance, this has led to a rekindled interest in phage therapy as an adjuvant or a replacement of antibiotic therapy against multi-resistant bacteria [11].

Virulent phages follow a strictly lytic cycle within their hosts, but they often exist in diverse communities with other virulent and temperate phages. Infection by the latter can lead to either the lytic cycle or their integration in bacterial genomes, as prophages (lysogenic cycle). Temperate phages are not used for phage therapy because lysogeny prevents them from extinguishing bacterial populations and confers resistance to closely, and sometimes distantly related phages – a mechanisms known as superinfection exclusion [12-14]. However, half of all bacterial genomes contain at least one, and up to 20, prophages, with these being more frequently found in bacterial pathogens [15], which means that they cannot be ignored in phage therapy. The expression of prophage genes may provide novel traits to the host (lysogenic conversion), and many cases have been described where prophages carry adaptive traits implicated in virulence or resistance to stress [16]. Virions arising from prophage induction can infect closely related competitor bacteria that are non-lysogenic for the phage, decreasing bacterial competition, increasing prophage

79 frequency, and liberating resources that can be used for the growth of the remaining lysogenic
80 population [17]. In this case, prophages have been regarded as weapons against bacterial
81 competitors [13,18].

82 Phages can drive horizontal gene transfer between bacteria by transduction [19]. This can be a
83 hazard in the case of phage therapy if the transferred traits are virulence factors or antibiotic
84 resistance genes. Specialized transduction occurs in temperate phages when prophage excision
85 leads to the transfer of neighboring chromosomal genes. Generalized transduction occurs when
86 bacterial DNA is delivered to other cells after being encapsulated in virions, due to the specificities
87 of the *pac* DNA packaging system [20]. Although these mechanisms are commonly used as
88 genetic engineering tools [21], they have been considered inevitable consequences of errors in
89 phage replication machineries and their rates in nature are poorly known. In the lab, they vary
90 across several orders of magnitude (between 10^{-11} and 10^{-3} [22,23]), depending on the phage, the
91 environment, and the type of culture media [19]. Importantly, phage driven transmission of
92 bacterial DNA can have particularly nefarious consequences for humans. Transducing phages are
93 responsible for the transmission of virulence factors in *Staphylococcus aureus* [24], and may
94 accelerate the spread of antibiotic resistance genes [25,26]. Transduction can also have an impact
95 at very short time scales: prophage induction facilitates the capture of adaptive traits (e.g., an
96 antibiotic resistance gene) from a second bacterial strain that is infected by the phage and, through
97 generalized transduction, transfers the gene back to the lysogenic strain. This process has been
98 called autotransduction [27]. Hence, phages drive the evolution of bacterial gene repertoires and
99 may spread virulence or antibiotic resistance factors during phage therapy.

100 The diversity of interactions between phages and bacteria may obscure the effects of each of
101 them. Experimental approaches have described and clarified the mechanisms underlying these
102 interactions, but usually focused on simplified environments [8,28]. *In vivo* studies of these
103 interactions (e.g., in mammalian hosts [29]) tackle more natural environments, but have limited

resolution in tracking temporal dynamics or the effects of individual mechanisms. Mathematical modelling provides a complementary approach to the study of phage-bacteria interactions, providing important insights on their co-evolutionary processes [30] or the dynamics of particular bacterial defense mechanisms [31,32]. Previous models have focused on individual mechanisms of interaction in simple environments (*e.g.*, how the evolution of resistance to phage can affect clinical treatments [33]), because tackling multiple mechanisms and spatial heterogeneity hinders the development of analytical solutions. Yet, natural communities, and particularly those relevant for phage therapy, include complex interactions and spatial structure [34-38]. This may explain why models sometimes fail to fully reproduce *in vivo* dynamics of phage infection [28], and why there is paucity of models on the impact of phage-mediated horizontal gene transfer in the adaptation of bacterial communities (but see the work of Volkova *et al.* [39] for a theoretical comparison between the relative efficacy of transduction versus conjugation in transmitting an adaptive trait).

Individual-based models (IBMs) are an alternative to population-based mathematical approaches for studying complex microbial systems [40]. They have been useful to understand, for instance, the effect of spatial structure in microbial social evolution [41] or the interactions between bacteria and virulent phages in biofilms [36]. Although computationally intensive, IBMs provide a framework to study biological systems through the incorporation of different (and potentially interacting) mechanisms at the level of the individual. Population-level dynamics can then emerge from the collective individual behaviors. This makes IBMs particularly appealing to investigate phage-bacteria interactions, because these involve both ecological (e.g., predation) and evolutionary (e.g., transduction of adaptive traits) scales, with antagonistic mechanisms defined at the individual level (e.g., the lysis-lysogeny decision of temperate phage). To study these multiple roles of phages in microbial communities, we developed an IBM approach that is able to simulate diverse mechanisms and eco-evolutionary contexts: eVIVALDI – eco-**eV**olutionary m**I**crobial

129 indi**V**idu**AL**-base**D** s**I**mulations. We focus on three questions, of gradually increasing complexity,
130 that are relevant for bacterial evolution and phage therapy, and that cover a range of possible eco-
131 evolutionary interactions between bacteria and phage. First, we introduce the basic scheme of the
132 simulation with the study of ecological interactions between co-evolving virulent phages and
133 bacteria under phage and antibiotic pressure in structured environments. Then we introduce
134 lysogeny and super-infection exclusion in the model to study the role of prophages as competitive
135 weapons. We show that our model provides better fit to previous experimental results than earlier
136 models. Finally, we introduce transduction and the way we encode individual genomes in the
137 model to elucidate how bacteria may obtain novel adaptive genes from sensitive bacteria by
138 autotransduction. We use eVIVALDI to explore and quantify the different mechanisms of phage-
139 bacteria interactions and to gain insights on how the structure of the environment can affect these
140 interactions and the community dynamics. We tackle each question by demonstrating the ability
141 of the model to capture previous results and then show how its complexity highlights new relevant
142 features.

143 # Methods

144 ## Concept and basic implementation

145 The eVIVALDI model was developed in Python (version 2.7.3), using an object-oriented approach,
146 with a focus on the flexibility and extensibility of mechanisms and parameters simulated. The
147 complete ODD (Overview, Design concepts, and Details) protocol [42] of the developed model is
148 available as supplementary text (Text S1, Table S1 has the parameters modelled and their
149 possible values), but below is a brief overview of the model. The source of the software can be
150 obtained in the following link: https://gitlab.pasteur.fr/jsousa/eVIVALDI. The simulations can be run
151 on a typical desktop computer. In a 3GHz 8-core Mac Pro, with 32GB of RAM, a replicate of a
152 simulation (100 iterations), takes from ~5 to 30 minutes, depending on the parameters.
153 Computations can also be performed in a cluster, allowing the parallel simulation of multiple
154 parameters.

155 ## Entities and their ecological setup

156 Both bacterial cells and phage particles are represented as independent individuals on an
157 environment represented as a two-dimensional grid with Moore neighbourhood (the 8 connected
158 grid spaces of each location, for a Moore distance of one) (Fig 1A). Bacteria can be of different
159 species. Each individual bacterium has a genome with core, accessory and, eventually, prophage
160 genes. Bacteria have individual phenotypes, such as growth rate or the ability to survive antibiotic
161 exposure. Phages can be from different species, have different lifestyles (temperate, virulent or
162 defective), and possess individual phenotypes (e.g., attachment receptors and burst sizes). The
163 host range of phage hosts is defined by a matrix (Fig 1B), and the superinfection exclusion rules
164 amongst phages is defined in a similar way (Fig 1C).

Environmental and bacterial updates

The environment and the individuals are updated and behave according to biologically inspired rules. The environment can be completely structured, semi-structured or not structured at all (i.e., well-mixed), and it can be set as bounded or have a toroidal space. The type of structure influences the diffusion of the different bacterial cells and environmental particles (phage and antibiotics). Each location can hold a single bacterial cell and several phage cells. Free space is the bacterial resource to be consumed, and it is freed whenever bacteria die. Bacterial death can be intrinsic (e.g., of old age) or explicit (e.g., exposure to antibiotics or predation by phage) (Fig 1D). When a free space is available, the neighboring bacteria compete for reproduction. The outcome of the competition is chosen through a roulette wheel method that accounts for the fitness of each bacterium. The successful bacterium generates an offspring into the free space (Fig 1E). Bacteria can be infected by phage in the environment. The outcome of the infection depends on the phage lifestyle and, for temperate phage, the lysis-lysogeny decision. This decision is stochastic but influenced by the number of surrounding phages. For temperate phage, integration in the host genome means vertical inheritance with host replication, until the phage excises from the genome, according to a probability that can be low but non-null throughout the simulation (stochastic prophage induction) and that can also be influenced by the level of antibiotic stress to which the host is exposed. Phage can transduce bacterial genes to other bacteria by generalized or specialized transduction (depending on phages' characteristics, Fig 1F).

Input, output and documentation of the model

The inputs of each simulation are two text files that define the general parameters and also the ecological setup of the environment (types and numbers of bacteria and/or phage, along with their attributes). The statistics collected at different time points are stored in dictionaries and dataframes (using *pandas*), can be tailored to the experimenter's choice and can be represented visually

189 (using *matplotlib* and *seaborn*) or created as an output file.

190 Random Forest Analysis

191 The Random Forest Analysis is based on simulations performed with the model, covering 3000
192 random combinations of parameters, with 30 simulated repeats per combination. The output of
193 this cohort of simulations is grouped and resumed in response variables, to which a column with
194 3000 rows of a random parameter is added (i.e., a choice of a number between 1 and 3). This
195 table is used as input of the randomForest package in R (version 4.6.12), where the *randomForest*
196 function is run with the parameters ntrees set to 10000. The relative importance of each parameter
197 (the percentage increase in minimum squared error, %IncMSE) is assessed using the *importance*
198 function from the same package.

199 Bacterial strains, antibiotics and growth conditions

200 Bacteria strains used in this study are listed in Table S2. Bacteria were grown in Tryptic Soy Broth
201 (TSB), Tryptic Soy Agar (TSA) and TSB+0,04%TSA from Oxiod. When appropriate, the following
202 antibiotics were applied: Erythromycin 10mg/L, Chloramphenicol 10 mg/L, Streptomycin 50 mg/L,
203 0.5 mg/L of Rifampicin. All antibiotics were purchased from Sigma.

204 Co-culture experiment

205 Cultures of JH944, JH927 and JH930 were incubated in 20ml TSB overnight with shaking (200
206 rpm) at 37◦C. OD600 was measured and cultures were diluted to final OD600 = 0.01 in 1:1 ratios
207 of JH944+JH930 and JH944+JH927 in TSB media supplemented with 5mM $CaCl_2$. After overnight
208 incubation (shaking 200 rpm at 37◦C), the cultures were sonicated (10 pulses, 500msec, 50%) to
209 ensure single bacterial cells when plating. Serially diluted cultures were plated on TSA containing
210 erythromycin (JH944+JH927) and chloramphenicol (JH944+JH930) and incubated overnight at
211 37◦C. The following day, 100 single colonies from the JH944+JH927 culture plates were streaked

212 on TSA supplemented with streptomycin and rifampicin, TSA supplemented with erythromycin
213 and TSA without addition. For the JH944+JH930 culture, 100 colonies were restreaked on TSA
214 supplemented with streptomycin and rifampicin, TSA supplemented with chloramphenicol and
215 TSA without addition. All plates were incubated overnight at 37◦C.

216 ## Phage induction assay

217 Bacteria lysogenic for phi11 were detected by a prophage induction assay. Bacterial colonies that
218 were present on TSA supplemented with chloramphenicol or erythromycin but absent on TSA
219 supplemented with streptomycin and rifampicin were selected for the phage induction assay. The
220 bacteria were inoculated in TSB and grown to mid-log phase (OD_{600} = 0.5) with shaking (200 rpm)
221 at 37◦C. Mitomycin C (Sigma) 0,4 mg/L was added to TSB to induce any prophages present in the
222 strain and the cultures were incubated at 37◦C with shaking (200 rpm) overnight. The cultures
223 were centrifuged at 4◦C, 3700 rpm for 10 min to pellet the cells and supernatant sterile filtered
224 (0.22 µm). Phages present in the supernatant were detected by mixing 100µl of the filtered
225 supernatant and 100µl of the indicator strain RN4220 in presence of 15µl 100mM $CaCl_2$. After
226 incubation at room temperature for 10 min, top agar (TSB+0,04%TSA) was added and the mixture
227 was poured onto a TSA plate supplemented with 10µM $CaCl_2$ and incubated at 37◦C overnight.
228 Phages present in the plates were indicative of the original culture being lysogenized by the phage.

229

230 **FIG 1. Mechanisms and workflow of the eVIVALDI model.** A) Bacterial cells and bacteriophage particles are modelled in a 2-
231 dimensional space, where each (x,y) location holds at most a single bacterial cell and at most a predefined maximum number of
232 phages. The environment ranges from completely well-mixed (liquid), where the contents of each location are randomized at each
233 iteration, to spatially structured, where they are fixed. An intermediate structure is achieved by allowing replication of bacterial cells
234 into a neighbourhood of a given distance. Bacteria and phage can be of different species, and the latter exist as entities either in the
235 environment, where they can infect new hosts, or within hosts, where they either replicate or integrate into their genomes. B) Phage
236 host range is defined in a matrix where each phage has a probability of infecting a given bacterial species. C) Superinfection exclusion
237 is the probability that infection by a given phage aborts when a given type of prophage is present. D) The basal probability of bacterial

238 death can increase by antibiotic exposure or phage infection. Phages decay in function of the period of time spent outside a bacterial
239 host. E) Bacteria compete to reproduce to empty locations, with the fittest bacteria being more likely to produce an offspring. The
240 offspring inherits the traits of the parent cell, but can undergo mutations and is placed into the free location. F) The type of phage
241 infection is determined by the lifestyle of the phage, with virulent following an obligatory lytic cycle, whilst temperate phage can
242 undertake the lytic or the lysogenic cycle following a stochastic decision affected by the density of phages in the environment. The
243 probability of specialized transduction is computed during excision, leading eventually to the incorporation into the phage DNA of a
244 neighboring gene. Generalized transduction occurs before the burst, and a virion has the probability to incorporate random genes from
245 its host, instead of its own DNA. Transduced genes can be used by the subsequently infected bacterial hosts. G) The main cycle of a
246 typical simulation within the model. See complete ODD in Supplementary Material.

247 # Results and Discussion

248 ## Ecology of phage-bacteria interactions in the light of antibiotic and phage therapy

249 Antimicrobial therapies rely on the effectiveness of selective agents to kill sensitive bacteria.
250 Phage therapy involves infection and reproduction of the killing agents, thus extending the ability
251 of standard chemical therapies. We started by investigating if eVIVALDI could reproduce simplified
252 but typical ecological scenarios where sensitive individuals are killed by antibiotics and/or predated
253 by virulent phages, thus promoting the increase in frequency of resistant bacteria. A simple
254 community of two bacterial species, one sensitive and another resistant (either to antibiotic or
255 virulent phage), was simulated in a well-mixed environment, and no new resistant bacterial
256 mutants were allowed to emerge in these simulations. Resistance can be defined as costly, in line
257 with experimental data [43], rendering resistant bacteria less competitive in the absence of
258 selection pressure (Fig S1). However, when either antibiotics (Fig 2A) or phage (Fig 2B) were
259 introduced in the environment, the resistant population rapidly increases to fixation. Predation by
260 phage leads to an initial increase in their numbers, because of the abundance of sensitive bacteria,
261 but also to their subsequent rapid extinction when sensitive hosts become unavailable (Fig 2B). A
262 combined treatment of antibiotics and virulent phages leads to the extinction of both populations
263 because none has the ability to survive both selective pressures (Fig 2C). However, the decrease
264 of the antibiotic sensitive population is slower in the presence of phages because of lower
265 competition from antibiotic resistant cells, which are killed by the phage (Fig S2A).

266 Our model allows to test explicitly the effect of spatial structure on community composition. Spatial
267 structure affects the ability of individuals to diffuse freely in the environment and is known to affect
268 population dynamics [35,36]. Here, spatially structured environments assume that bacteria are
269 fixed in their locations, and can divide only to their immediately adjacent locations. Likewise, we
270 assume that, in these environments, phage cannot diffuse, and thus can only propagate by

271 infecting nearby bacteria. Antibiotics applied homogeneously in spatially structured communities
272 delay the extinction of the sensitive bacteria in comparison to non-structured environments (Fig
273 S2B). However, antibiotics are more likely to be applied non-homogeneously when environments
274 are structured. The delayed extinction is more pronounced in these conditions leading to long term
275 coexistence between sensitive and resistance bacteria (Fig S3). The effect of phage predation on
276 community dynamics is markedly different between well-mixed and spatially structured
277 environments because the latter decreases dispersion leading to "predation waves" that produce
278 spatial arrangements of dead cells akin to those observed in phage plaque assays (see Fig S4
279 and Video S1). Ultimately, spatial structure results in delayed extinction of phage susceptible cells
280 (Fig 2E vs Fig 2B). Similar to well-mixed environments, presence of antibiotics and phage in
281 spatially structured environments leads to a much slower extinction of antibiotic resistant bacteria
282 compared to environments with antibiotics but lacking phages (Fig 2F vs Fig 2D). However, the
283 presence of phages and antibiotics in spatially structured environments leads to a faster extinction
284 of antibiotic sensitive populations, compared to well mixed environments (Fig 2F vs Fig 2C, Fig
285 S2C), due to a much less efficient phage predation of their competitors when the environment is
286 structured.

287

288 **Fig 2. Community dynamics driven by antibiotic selection and phage predation.** A small community composed of two different
289 species is subjected to different selective pressures. Bacteria can be sensitive to antibiotics but resistant to phage (in green), or
290 resistant to antibiotics but sensitive to phage (in red). We follow the temporal dynamics and show the populations in their respective
291 colors (the number of free phage in the environment is shown in black). Solid lines indicate mean values for 30 simulations ran with
292 the same parameters and shaded areas show their 95% confidence interval. At the right of each plot is a representative time lapse at
293 3 time points of the lattices for each scenario, where the colors represent each bacterial species and white spaces represent the
294 absence of bacterial cells. In A) and D) antibiotics are applied at the indicated time. In B) and E), virulent phages (10 individual particles)
295 are co-inoculated with the bacteria at time 0. In C) and F), both selective regimes are applied, with antibiotics applied at the indicated
296 time and virulent phage co-inoculated with bacteria at time 0. In A), B) and C), the environment is homogeneous (well-mixed), as in
297 liquid culture. In D), E) and F), the environment is spatially structured. In D) and F) antibiotics are applied homogenously in the

298 structured environment, and in E) and F) each of the 10 phage particles is initially placed randomly in the biofilm. The complete set of
299 parameters for these simulations is show in supplementary data.

300

301 The introduction of mutations in the model, eventually reversing the susceptibility to antibiotics or
302 phages, tends to stabilize the bacterial populations (Fig S5A-B). Nevertheless, some populations
303 still go extinct because of the loss of rare mutants by genetic drift or because no adaptive
304 mutations occurred in the time span. Under pressure of antibiotics and phages, double resistant
305 cells emerge only when the mutation rate is very high (Fig S5C). The impact of the environmental
306 structure in the dynamics of predation (Fig 2) led us to analyze how it affects the emergence of
307 resistant lineages (Fig 3). Whilst single resistant mutants increase in frequency slower in
308 structured environments (Fig S5D), double mutants resistant to antibiotics and phage are much
309 more likely to emerge (Fig 3A-D) for intermediate rates of mutation (Fig 3E). This is because in
310 structured environments, the rare mutants resistant to antibiotics benefit from the resources
311 available from neighboring dead cells and rise in frequency without contact with phages (that
312 diffuse less efficiently). This increases the span of time available for the acquisition of secondary
313 mutations conferring resistance to phages, especially if the initial number of phages is not very
314 high (Fig S6). Hence, the acquisition of multiple adaptive mutations is more likely to occur in
315 structured environments.

316

317 **Fig 3. Spatial structure promotes the emergence of multi-resistant bacteria.** A-D) Simulations of a single bacterial species, initially
318 sensitive to antibiotics and phage. Lines show 30 replicate simulations with emerging resistant lineages (to one or both selective
319 pressures). Single mutants resistant to phage are shown in red, whilst single mutants resistant to bacteria are shown in green. Double
320 mutant lineages resistant to antibiotics and phage are shown in grey. In A) and B) mutants emerge at a rate of 10^{-4}. C and D) mutants
321 emerge at a rate of 10^{-3}. A and C show dynamics from well-mixed environments. B and D show dynamics from spatially structured
322 environments. E) Percentage of simulations (out of 30) where lineages resistant both to antibiotics and phage have emerged, in either
323 well mixed or spatially structured environments, for all the mutation rates tested (x-axis). The complete set of parameters for these

simulations is show in supplementary data.

The ability of bacteria to evolve resistance to phage might be futile if phage can also adapt sufficiently fast to overcome these changes [44]. When we allowed bacteria *and* phage to evolve in our simulations (Fig S7A), we observed co-evolutionary arms races similar to both theoretical expectations [33] and experimental observations [45]. Spatially structured environments showed slower co-evolution dynamics and higher variability between simulations than well-mixed ones (Fig S7B). Heterogeneous antibiotics added in structured environments further delayed the co-evolution dynamics (Fig S7C-D), due to the death of a significant part of the bacterial population. Importantly, and as before (Fig 3), surviving bacteria (either resistant to antibiotics or not exposed to lethal concentrations) were able to generate mutants resistant to phages for a longer period of time. This is not only due to the limited diffusion of phage, but also because phages need bacterial hosts to replicate and to generate their own genetic diversity. Thus, a reduction in the number of bacterial hosts due to antibiotic exposure hinders both phage propagation and evolution. This suggests that, in natural environments, multiple stressors might render co-evolutionary arms races less predictable than proposed by theoretical models and experimental settings that assume homogeneous populations and environments.

Lysogeny as a weapon

Contrary to virulent phages, temperate phages may integrate the bacterial host genome and reproduce vertically with it. The lysis-lysogeny decision in our simulations mimics experimental observations [46], and is influenced by the amount of competition faced by the phage: lysogeny is more likely under high viral concentrations or high multiplicity of infection (Fig S8). Since lysogens are protected from further infections by similar phages, due to superinfection exclusion, the environmental concentration of phages in the simulations decreases rapidly with the increase of

348 lysogens (and depending on free phage half-life). When lysogeny occurs mostly at high viral
349 concentration the bacterial population can become extinct before lysogens can arise.
350 Theoretically, this can also result in the extinction of the phage population.

351 When a lysogen invader arrives at a community with resident bacteria sensitive to its prophage,
352 lysis of a small fraction of the invaders can dramatically reduce the population of resident sensitive
353 bacteria. This liberates resources for the lysogenic invaders [13]. eVIVALDI recapitulates previous
354 experimental data on this prophage-as-a-weapon hypothesis [17] (Fig 4a): prophage induction
355 rapidly decreases the sensitive population of residents in the early stages of the process, but
356 lysogenization of the latter rapidly neutralizes this process (because the resident lysogens are
357 now resistant to the phage). Hence, the use of prophages as a biological weapon can provide a
358 decisive advantage for colonizing a new niche, but is rapidly neutralized by lysogenization of
359 competitor bacteria. This is also in agreement with previous theoretical works exploring dynamics
360 of invasion in well-mixed environments, using prophages as a competitive weapon [47].

361 The advantage of lysogens in the colonization of an environment of resident sensitive bacteria
362 was recently demonstrated in the mouse gut and was suggested to depend on the initial ratio
363 between invaders and resident cells [29]. Indeed, our simulations considering different initial ratios
364 of invading lysogens versus resident non-lysogens showed that the latter were more likely to
365 survive as lysogens when more abundant in the beginning of the process (Fig S9). The
366 abovementioned study presented a population-based mathematical model that fitted well most
367 experimental data, but predicted faster initial infection rates than the observed ones. While
368 different parameters can slow down these dynamics (e.g., the burst size of the phage [29]), the
369 spatially structured mouse gastrointestinal tract is likely to interfere with the temporal dynamics of
370 lysogeny. Interestingly, the inclusion of spatial structure in our model, absent from the
371 abovementioned models, led to a slower increase of free viral particles and slower generation of
372 lysogens in the resident strain (Fig 4B-C). This implicates that invading lysogens may be more

successful *in vivo* than would have been predicted by *in vitro* studies in well-mixed environments.

Fig 4. The role of lysogeny in community dynamics. A) Genomes from species A (invaders, grey bars) carry an inducible prophage, whereas those of species B (residents, white bars) are initially non-lysogens. Species are co-inoculated at a 1:10 mixture. Phages (black lines) are spontaneously induced from the lysogenic population. These phages infect the sensitive resident population, which may form lysogens that are protected from phages (B*, black bars). Eventually, the resident that are not lysogens become extinct. All bars represent the average of 30 replicate simulations with similar parameters, with the error bars indicating their 95% confidence interval. Data was displayed as in Figure 1 of [17] for comparison. B) Invading lysogens (L, red lines) and resident sensitive cells (S, blue lines) are co-inoculated at a ratio of 1:10. Phages (purple lines) are spontaneously induced and generate new lysogens in the sensitive resident cells (S^L, green lines). Full lines: well-mixed environments. Dashed lines: spatially structured environment. Data was displayed as in Figure 3 of [29] for comparison. C) Emergence of resident lysogens in well-mixed (blue) and in spatially structured (orange) environments during the initial 10 iterations of the simulations shown in B. Shown is the polynomial fit of order 2 for the initial 10 iterations, for each of the two types of environment; ANCOVA between the two environments, F=485.5, p=0. The complete set of parameters for these simulations is show in supplementary data.

Autotransduction of an antibiotic resistance gene

When the phages lysing the resident sensitive cells are capable of generalized transduction, they can transfer adaptive traits back to the invader lysogens (autotransduction [27], Fig 5A). To study this process, we started by demonstrating the adaptive effect of lysogenic conversion in bacteria and how it can impact the competition between different phages (Fig S10). We recreated the conditions for autotransduction within our model, by introducing two strains with similar initial population sizes: a non-lysogenic strain resistant to antibiotics ("residents") and a strain of lysogenic antibiotic sensitive "invaders" (Fig 5A). After initial growth, antibiotics are applied in the environment and, as in the experimental study [27], the invaders survive because they acquire the resistance gene by generalized transduction (Fig 5A-B). The analysis of the bacterial genomes in the simulations indicates multiple successive transduction events from the resident to the invader cells (Fig 5C). These events are random (i.e., transduction can transfer any part of bacterial DNA),

400 but natural selection results in over-representation of those transferring antibiotic resistance
401 genes. Overall, invaders lead residents to extinction in most simulations (62%), but sometimes
402 residents become lysogens and outcompete invaders (3%). Interestingly, many simulations
403 exhibited coexistence of lysogenic invaders and lysogenic residents (22%, Fig 5D), and a few
404 showed extinction of all bacterial populations (13%).

405

406 **Fig 5. Simulation of autotransduction.** A) Representation of the autotransduction events. We created a multispecies community akin
407 to the experimental work of [27], where the invader lysogenic species (red) is sensitive to antibiotics and the resident non-lysogenic
408 species (green) is resistant to antibiotics but sensitive to the phage of the invaders. B) Temporal dynamics of a typical simulation
409 leading to the survival of the invaders. The black line indicates the number of phages in the environment and the time of application of
410 antibiotics is indicated with the grey line. C) Samples of genomes in the population at two different time points of the simulations of
411 panel B. Before antibiotics (*t=2*), the genomes of the resident population (green) carry the resistance trait (orange marker). The invader
412 population (red) is not resistant (grey marker indicates sensitivity to drugs). After the application of antibiotic (*t=10*) most of the invaders
413 have the original prophage and a random sequence of bacterial DNA transduced from the resident cells (other ellipses). D) Outcome
414 of 100 simulations. The complete set of parameters for these simulations is show in supplementary data.

415

416 eVIVALDI includes many complex stochastic mechanisms and it is not straightforward to
417 empirically disentangle the importance of each in the final outcome. Therefore, we used a machine
418 learning approach, Random Forest Analysis (RFA, see Methods), to quantify the importance of
419 the mechanisms driving the increase of the population of invaders (Fig 6A, in File S7 are the
420 parameters explored with the RFA). We focused on the percentage increase in minimum squared
421 error (MSE) associated with each variable in the simulation. Generalized transduction had the
422 strongest effect in the efficiency of autotransduction (86% increase in mean square error [MSE],
423 Fig 6B), whilst specialized transduction was almost negligible (3% increase in MSE).
424 Autotransduction also improved with higher probability of adsorption (44% increase in MSE) and
425 infection distance (i.e., the maximum distance between a bacterium and a phage still allowing

426 infection, 70% increase in MSE), because they increase the reach and efficiency of infection by
427 phage and, subsequently, the likelihood of generalized transduction (Fig 6C, Fig S11B). In
428 contrast, when the decision to enter lysogeny (49% increase in MSE) can be made with high
429 probability for relatively low viral concentrations, the resident population proliferates (Fig S11D
430 and Fig S11I for the lysis-lysogeny decision functions explored with the RFA). The importance of
431 the remaining parameters is detailed in Fig S11.

432

433 **Fig 6. Identification of the main mechanisms affecting the rate of autotransduction of an antibiotic resistance gene using**
434 **Random Forest Analysis.** A) Analysis is based on 3000 randomized combinations of parameters and 30 repeated simulations for
435 each combination). Parameters with a higher % in increased minimum square error have a higher importance for the measured
436 outcome: the median of the final relative frequency of the invader. A random parameter (in grey) was included in the analysis to provide
437 a baseline reference of importance. B-C) The directionality of the impact of two parameters is assessed by plotting the frequency of
438 the invader population at the end of the simulation (across all simulations), in function of the parameter of interest (the other parameters
439 are shown in Fig S11). In the left y-axis, and as strip plot of grey dots, is the distribution of the frequency of the invader population in
440 all simulations. In the right y-axis, and as red dots and lines, is the median of this frequency across the simulations.

441

442 To better understand the relationship between two of the most important parameters, generalized
443 transduction and probability of phage attachment, we explored their space of parameters at a
444 higher resolution than before (Fig 7A), while fixing all other parameters. We found that a critical
445 combination of high adsorption efficiency (>1%) and high (between 0.01% and 80%) probability
446 of generalized transduction is required for the survival of invaders (red region). The survival of the
447 resident population is the most likely outcome when rates of transduction and/or infection are low,
448 but also when all phages engage in generalized transduction (100% probability of generalized
449 transduction), because in this case no viable particles are released in the environment (green
450 region). The space of parameters leading to coexistence (yellow region) separates the region
451 leading to the overrepresentation of the invaders from the one leading to the overrepresentation

452 of the resident species (see also Fig S12).

453 The study describing the discovery of autotransduction focused on the process of gene acquisition
454 by the invaders and did not address the possibility of co-existence [27]. We thus experimentally
455 addressed the prediction of co-existence by co-culturing in liquid media supplemented with
456 chloramphenicol two strains of *Staphylococcus aureus*: a lysogenic strain (JH944, "invaders")
457 sensitive to the antibiotic and either one of two non-lysogenic strains (JH930 or JH927, "residents")
458 resistant to the antibiotic (see Methods). The two different resident strains were chosen to
459 demonstrate the result both in the laboratory strain 8325-4 (JH930) as well as in the clinically more
460 relevant strain USA300 (JH927) background. The majority of the colonies resistant to
461 chloramphenicol isolated at the end of the two experiments are in the JH944 background,
462 indicating the acquisition of the resistance gene from the resident bacteria by autotransduction.
463 However, in both combination of strains, performed in 3 biological replicates, a subpopulation of
464 JH927 (17.3±1.1%) or JH930 (31.3±6.7%), respectively, were observed to coexist with the invader
465 strain (Fig 7B, Table S3), confirming our predictions. Interestingly, in simulations were coexistence
466 is frequently observed, the frequency of invaders can be influenced by both the probability of
467 adsorption and the probability of generalized transduction (Fig S13). The different frequencies of
468 invaders observed in co-culture with either JH927 or JH930 could represent different regions of
469 the predicted parameter space, where released phages have, for instance, a higher infection
470 efficiency towards JH927 compared to JH930. Confirmation of this hypothesis will require further
471 work on the biology of these phages. Importantly, we observed in the simulations that coexistence
472 is strictly dependent on the generation of lysogenic variants of the resident bacteria, being
473 suppressed when we performed simulations without the generation of new lysogens (Fig S14A-
474 D). This is experimentally corroborated with the observed release of phage particles from the
475 surviving resident clones at the end of the co-culture, when these are exposed to mitomycin C
476 (Fig 7B, Table S3, see Methods). This confirms that lysogenization of the resident bacteria is the

477 mechanism responsible for the coexistence between the two strains and validates the predictions
478 of the model.

479 Our simulations further suggest that structured environments (Fig S12A) provide an additional
480 region, for extremely high rates of transduction, where coexistence is prevalent (upper regions in
481 Fig S12B-C). These high rates are biologically implausible for viable phages, but not for defective
482 phages or for gene transfer agents [48]. Finally, extinctions of both strains were more frequent
483 when the probability of adsorption was high and transduction was low, suggesting that an inducible
484 phage that is highly infective but a poor transducer is more likely to lead to the collapse of both
485 the invaders and the antibiotic resistant populations. The likelihood of double extinctions is higher
486 in structured environments (Fig S12A, Fig S15 and Fig S16) or in the absence of lysogenization
487 of the resident bacteria (Fig S14E-F and Fig S17). Our results suggest that ecological interactions
488 between strains invading communities of susceptible bacteria can be very diverse, depending on
489 the rates of infection, transduction, lysogenization and population structure.

490

491 **Fig 7. The combined role of probability of adsorption and generalized transduction for the autotransduction of an antibiotic**
492 **resistance gene.** The simulation scenario is similar to Fig 6. **A)** The heatmap represents the likelihood of the outcome of the
493 simulations in function of the two parameters. The color scale ranges from green (100% of the final population composed resident
494 bacteria) to red (100% of the final population composed of invader bacteria), with yellow regions indicating cases where coexistence
495 is the outcome more likely to occur in the timeframe of the simulations. 30 repeat simulations were performed for each combination of
496 parameters, and their median value is used to construct the heatmap. When both populations went extinct, this was either ignored to
497 compute the median (if it occurred in less than 50% of the cases), or was marked as grey (otherwise). **B)** Co-cultures of a lysogenic
498 chloramphenicol sensitive strain of *S. aureus* (JH944, "invaders", red) and a non-lysogenic chloramphenicol resistant strain (JH930 or
499 JH927, "residents", green or green with white circles, respectively) indicate coexistence between the two strains at the end of the
500 experiment. Y-axis shows the percentage of colonies with a given genotype (out of 100 or 127 in total, for co-cultures with JH930 or
501 JH927, respectively). Each stacked bar represents an independent replicate of the experiment.

502

Conclusion

Individual-based modelling is providing novel ways to analyze and predict the behavior of microbial systems [40]. Our novel approach integrates multiple and different bacterial species, phages, environmental structures and ecological conditions to explore different aspects of bacteria-phage interactions: temporal changes in community composition (e.g., between lysogens and non-lysogenic bacteria), the concurrent effects of mechanisms of infection, lysogeny, and transduction, and their consequences for the genomic composition of each individual bacteria and phage. To the best of our knowledge, no other theoretical or computation model integrates these different scales of phage-bacteria interactions. This has allowed us to characterize and quantify key ecological components, such as structured environments, in the dynamics emerging from these interactions.

Models are based on simplifying assumptions to make biological systems more tractable. This facilitates pinpointing the relevance of certain mechanisms or agents, but may result in misleading over-simplifications of the system. One major difference between biological systems and our model concerns the number of cells which, due to computational reasons, is lower than the one typically used in experimental settings. Even though our results are qualitatively similar to experimental and/or other theoretical works, this difference may affect the quantitative results. The decreased effective population size (and the consequent increase in the effect of drift) requires that certain rates (e.g., mutation or transduction rates) are simulated at higher values, in order to increase the probability of detecting such events. Another limitation lies in the characterization of the environment. Even if we allow for different levels of structure, environments are spatially and temporally constant throughout the simulations, which might not always be the case in nature. This can change the dynamics of propagation of phages, and lead to subpopulations specialized for different spatial niches. A third limitation of the model lies on the lack of a true physiological

527 description of the bacteria. We assume that phages can infect bacteria at any time, but phage
528 infectivity is known, in some cases, to depend on whether its bacterial host is in exponential or
529 stationary phase [49]. In other cases, a stochastic or induced persistence state in bacteria allows
530 the population to maintain alive a sensitive subpopulation [50]. This can lead to a slowdown or
531 complete halt of infection, particularly in structured environments. Nevertheless, it is important to
532 underline that the model was designed to be easily extensible and further assimilate new
533 mechanisms. Some that are already implemented but not thoroughly explored here include phage
534 resistance based on adaptive immunity (e.g., CRISPR-Cas [32,51]) or mutations affecting the
535 phage host range [52].

536 One of the major conclusions of this work is that spatial structure affects the dynamics of bacterial
537 populations in the face of antibiotic exposure, phage predation or a combination of both. Whilst
538 combining phages and antibiotics is one of the proposed strategies for the clinical use of phage
539 [53,54], we show here that the emergence of bacteria resistant to both stressors can be enhanced
540 by structured environments, particularly when antibiotics are not homogeneously distributed, as
541 seems common in natural settings [55,56]. This should be taken into account in phage therapy
542 studies.

543 Adaptation of bacterial cells can also be driven by temperate phage. We showed how
544 autotransduction promotes the spread of antibiotic resistance and is affected by different
545 mechanisms. Importantly, we predicted that different community outcomes (coexistence and
546 extinction) can occur by modulating the efficiency of phages' infection, lysogeny and transduction,
547 as well as the structure of the environment. We experimentally confirmed the emergence of co-
548 existence between strains of *S. aureus* in well mixed environments, underlining the power of our
549 approach in generating valid and testable hypotheses. It will be important to further test its
550 predictions, as well to simulate other ecologically (and clinically) relevant scenarios. In particular,
551 it will be crucial to explore how the co-existence between virulent phages and prophages

552 influences the outcomes of a combined treatment with phage and antibiotics under a range of
553 ecological interactions between the two types of phages. Exploring these and other ecological
554 settings is also key to understand which factors impact the evolutionary consequences of phage-
555 bacteria interactions for microbial populations.

556

557 ACKNOWLEDGEMENTS

558 We thank Marie Touchon and José Pénadés for comments, suggestions, and criticisms during the
559 development and testing of the model. This work was funded by European Research Council grant
560 [EVOMOBILOME n°281605] to E.P.C.R. and by an EU FP7 PRESTIGE grant [PRESTIGE-2017-
561 1-0012] from Campus France to J.A.M.S. H.I. is supported by the Danish National Research
562 Foundation's Centre of Excellence Bacterial Stress Response and Persistence (DNRF12) and
563 J.H. is supported by a Young Elite Researcher grant from the Danish Research Council, Sapere
564 Aude.

565

566 REFERENCES

567 1. Didelot X, Walker AS, Peto TE, Crook DW, Wilson DJ. Within-host evolution of bacterial
568 pathogens. Nat Rev Micro. 2016;14: 150–162. doi:10.1038/nrmicro.2015.13

569 2. Brooks AW, Kohl KD, Brucker RM, van Opstal EJ, Bordenstein SR. Phylosymbiosis:
570 Relationships and Functional Effects of Microbial Communities across Host Evolutionary
571 History. PLoS Biol. 2016;14: e2000225–29. doi:10.1371/journal.pbio.2000225

572 3. Fuhrman JA. Marine viruses and their biogeochemical and ecological effects. Nature.
573 1999;399: 541–548. doi:10.1038/21119

574 4. Koskella B, Brockhurst MA. Bacteria-phage coevolution as a driver of ecological and
575 evolutionary processes in microbial communities. FEMS Microbiol Rev. 2014;38: 916–
576 931. doi:10.1111/1574-6976.12072

577 5. Perfeito L, Fernandes L, Mota C, Gordo I. Adaptive mutations in bacteria: high rate and
578 small effects. Science. 2007;317: 813–815. doi:10.1126/science.1142284

579 6. Ghoul M, Mitri S. The Ecology and Evolution of Microbial Competition. Trends Microbiol.
580 2016;24: 833–845. doi:10.1016/j.tim.2016.06.011

581 7. Engelhardt T, Kallmeyer J, Cypionka H, Engelen B. High virus-to-cell ratios indicate
582 ongoing production of viruses in deep subsurface sediments. ISME J. 2014;8: 1503–
583 1509. doi:10.1038/ismej.2013.245

584 8. Díaz-Muñoz SL, Koskella B. Bacteria-phage interactions in natural environments. Adv
585 Appl Microbiol. Elsevier; 2014;89: 135–183. doi:10.1016/B978-0-12-800259-9.00004-4

586 9. Clokie MR, Millard AD, Letarov AV, Heaphy S. Phages in nature. Bacteriophage. 2011;1:
587 31–45. doi:10.4161/bact.1.1.14942

588 10. Suttle CA. Marine viruses--major players in the global ecosystem. Nat Rev Micro. 2007;5:
589 801–812. doi:10.1038/nrmicro1750

590 11. Roach DR, Debarbieux L. Phage therapy: awakening a sleeping giant. Emerg Top Life
591 Sci. 2017;1: 93–103. doi:10.1042/ETLS20170002

592 12. Susskind MM, Botstein D, Wright A. Superinfection exclusion by P22 prophage in
593 lysogens of Salmonella typhimurium. III. Failure of superinfecting phage DNA to enter
594 sieA+ lysogens. Virology. 1974;62: 350–366.

595 13. Harrison E, Brockhurst MA. Ecological and Evolutionary Benefits of Temperate Phage:
596 What Does or Doesn't Kill You Makes You Stronger. Bioessays. 2017;197: 1700112.
597 doi:10.1002/bies.201700112

598 14. Bondy-Denomy J, Qian J, Westra ER, Buckling A, Guttman DS, Davidson AR, et al.
599 Prophages mediate defense against phage infection through diverse mechanisms. ISME
600 J. 2016;10: 2854–2866. doi:10.1038/ismej.2016.79

601 15. Touchon M, Bernheim A, Rocha EP. Genetic and life-history traits associated with the
602 distribution of prophages in bacteria. ISME J. 2016. doi:10.1038/ismej.2016.47

603 16. Brüssow H, Canchaya C, Hardt W-D. Phages and the evolution of bacterial pathogens:
604 from genomic rearrangements to lysogenic conversion. Microbiol Mol Biol Rev. 2004;68:
605 560–602. doi:10.1128/MMBR.68.3.560-602.2004

606 17. Bossi L, Fuentes JA, Mora G, Figueroa-Bossi N. Prophage contribution to bacterial
607 population dynamics. J Bacteriol. 2003;185: 6467–6471. doi:10.1128/JB.185.21.6467-
608 6471.2003

609 18. Gama JA, Reis AM, Domingues I, Mendes-Soares H, Matos AM, Dionisio F. Temperate
610 bacterial viruses as double-edged swords in bacterial warfare. PLoS ONE. 2013;8:
611 e59043. doi:10.1371/journal.pone.0059043

612 19. Touchon M, Moura de Sousa JA, Rocha EP. Embracing the enemy: the diversification of
613 microbial gene repertoires by phage-mediated horizontal gene transfer. Curr Opin
614 Microbiol. 2017;38: 66–73. doi:10.1016/j.mib.2017.04.010

615 20. Weinstock GM. Transduction in Gram-Negative Bacteria. Modern Microbial Genetics.

616 2002. pp. 561–579. doi:10.1002/047122197X.ch21

617 21. Henry M, Debarbieux L. Tools from viruses: bacteriophage successes and beyond.
618 Virology. 2012;434: 151–161. doi:10.1016/j.virol.2012.09.017

619 22. Kenzaka T, Tani K, Sakotani A, Yamaguchi N, Nasu M. High-frequency phage-mediated
620 gene transfer among Escherichia coli cells, determined at the single-cell level. Appl
621 Environ Microbiol. 2007;73: 3291–3299. doi:10.1128/AEM.02890-06

622 23. Kenzaka T, Tani K, Nasu M. High-frequency phage-mediated gene transfer in freshwater
623 environments determined at single-cell level. ISME J. 2010;4: 648–659.
624 doi:10.1038/ismej.2009.145

625 24. Xia G, Wolz C. Phages of Staphylococcus aureus and their impact on host evolution.
626 Infect Genet Evol. 2014;21: 593–601. doi:10.1016/j.meegid.2013.04.022

627 25. Balcazar JL. Bacteriophages as Vehicles for Antibiotic Resistance Genes in the
628 Environment. Miller V, editor. PLoS Pathog. 2014;10: e1004219–4.
629 doi:10.1371/journal.ppat.1004219

630 26. Haaber J, Penadés JR, Ingmer H. Transfer of Antibiotic Resistance in Staphylococcus
631 aureus. Trends Microbiol. 2017;25: 1–13. doi:10.1016/j.tim.2017.05.011

632 27. Haaber J, Leisner JORJ, Cohn MT, Catalan-Moreno A, Nielsen JB, Westh H, et al.
633 Bacterial viruses enable their host to acquire antibiotic resistance genes from
634 neighbouring cells. Nat Commun. 2016;7: 1–8. doi:10.1038/ncomms13333

635 28. Bull JJ, Gill JJ. The habits of highly effective phages: population dynamics as a
636 framework for identifying therapeutic phages. Front Microbiol. 2014;5: 1–12.
637 doi:10.3389/fmicb.2014.00618

638 29. De Paepe M, Tournier L, Moncaut E, Son O, Langella P, Petit M-A. Carriage of λ Latent
639 Virus Is Costly for Its Bacterial Host due to Frequent Reactivation in Monoxenic Mouse
640 Intestine. PLoS Genet. 2016;12: e1005861. doi:10.1371/journal.pgen.1005861

641 30. Weitz JS, Hartman H, Levin SA. Coevolutionary arms races between bacteria and
642 bacteriophage. Proc Natl Acad Sci USA. 2005;102: 9535–9540.
643 doi:10.1073/pnas.0504062102

644 31. Berngruber TW, Lion S, Gandon S. Evolution of suicide as a defence strategy against
645 pathogens in a spatially structured environment. Ecol Lett. 2013;16: 446–453.
646 doi:10.1111/ele.12064

647 32. Koonin EV, Wolf YI. Evolution of the CRISPR-Cas adaptive immunity systems in
648 prokaryotes: models and observations on virus-host coevolution. Mol Biosyst. 2014;11:
649 20–27. doi:10.1039/C4MB00438H

650 33. Levin BR, Bull JJ. Population and evolutionary dynamics of phage therapy. Nat Rev
651 Micro. 2004;2: 166–173. doi:10.1038/nrmicro822

652 34. McVay CS, Velásquez M, Fralick JA. Phage therapy of Pseudomonas aeruginosa

653 infection in a mouse burn wound model. Antimicrob Agents Chemother. 2007;51: 1934–
654 1938. doi:10.1128/AAC.01028-06

655 35. Brockhurst MA, Buckling A, Rainey PB. Spatial heterogeneity and the stability of host-
656 parasite coexistence. J Evol Biol. 2006;19: 374–379. doi:10.1111/j.1420-
657 9101.2005.01026.x

658 36. Simmons M, Drescher K, Nadell CD, Bucci V. Phage mobility is a core determinant of
659 phage-bacteria coexistence in biofilms. ISME J. 2017;89: 135.
660 doi:10.1038/ismej.2017.190

661 37. Roach DR, Leung CY, Henry M, Morello E, Singh D, Di Santo JP, et al. Synergy between
662 the Host Immune System and Bacteriophage Is Essential for Successful Phage Therapy
663 against an Acute Respiratory Pathogen. Cell Host Microbe. 2017;22: 38–47.e4.
664 doi:10.1016/j.chom.2017.06.018

665 38. Barr JJ. A bacteriophages journey through the human body. Immunol Rev. 2017;279:
666 106–122. doi:10.1111/imr.12565

667 39. Volkova VV, Lu Z, Besser T, Gröhn YT. Modeling the infection dynamics of
668 bacteriophages in enteric Escherichia coli: estimating the contribution of transduction to
669 antimicrobial gene spread. Appl Environ Microbiol. 2014;80: 4350–4362.
670 doi:10.1128/AEM.00446-14

671 40. Hellweger FL, Clegg RJ, Clark JR, Plugge CM, Kreft J-U. Advancing microbial sciences
672 by individual-based modelling. Nat Rev Micro. 2016;14: 461–471.
673 doi:10.1038/nrmicro.2016.62

674 41. Nadell CD, Foster KR, Xavier JB. Emergence of Spatial Structure in Cell Groups and the
675 Evolution of Cooperation. PLoS Comput Biol. 2010;6: e1000716–9.
676 doi:10.1371/journal.pcbi.1000716

677 42. Grimm V, Berger U, Bastiansen F, Eliassen S, Ginot V, Giske J, et al. A standard protocol
678 for describing individual-based and agent-based models. Ecol Modell. 2006;198: 115–
679 126. doi:10.1016/j.ecolmodel.2006.04.023

680 43. Andersson DI, Levin BR. The biological cost of antibiotic resistance. Curr Opin Microbiol.
681 1999;2: 489–493.

682 44. Samson JE, Magadán AH, Sabri M, Moineau S. Revenge of the phages: defeating
683 bacterial defences. Nat Rev Micro. 2013;11: 1–13. doi:10.1038/nrmicro3096

684 45. Gómez P, Ashby B, Buckling A. Population mixing promotes arms race host-parasite
685 coevolution. Proc Biol Sci. 2015;282: 20142297–20142297. doi:10.1098/rspb.2014.2297

686 46. Zeng L, Skinner SO, Zong C, Sippy J, Feiss M, Golding I. Decision making at a
687 subcellular level determines the outcome of bacteriophage infection. Cell. 2010;141: 682–
688 691. doi:10.1016/j.cell.2010.03.034

689 47. Brown SP, Le Chat L, De Paepe M, Taddei F. Ecology of microbial invasions:
690 amplification allows virus carriers to invade more rapidly when rare. Curr Biol. 2006;16:

691 2048–2052. doi:10.1016/j.cub.2006.08.089

692 48. Lang AS, Westbye AB, Beatty JT. The Distribution, Evolution, and Roles of Gene Transfer
693 Agents in Prokaryotic Genetic Exchange. Annu Rev Virol. 2017;4: 87–104.
694 doi:10.1146/annurev-virology-101416-041624

695 49. Chibani-Chennoufi S, Bruttin A, Dillmann M-L, Brüssow H. Phage-host interaction: an
696 ecological perspective. J Bacteriol. American Society for Microbiology; 2004;186: 3677–
697 3686. doi:10.1128/JB.186.12.3677-3686.2004

698 50. Chapman-McQuiston E, Wu XL. Stochastic receptor expression allows sensitive bacteria
699 to evade phage attack. Part I: experiments. Biophys J. 2008;94: 4525–4536.
700 doi:10.1529/biophysj.107.120212

701 51. Bradde S, Vucelja M, Teşileanu T, Balasubramanian V. Dynamics of adaptive immunity
702 against phage in bacterial populations. PLoS Comput Biol. 2017;13: e1005486–16.
703 doi:10.1371/journal.pcbi.1005486

704 52. De Sordi L, Khanna V, Debarbieux L. The Gut Microbiota Facilitates Drifts in the Genetic
705 Diversity and Infectivity of Bacterial Viruses. Cell Host Microbe. 2017;22: 801–808.e3.
706 doi:10.1016/j.chom.2017.10.010

707 53. Torres-Barceló C, Hochberg ME. Evolutionary Rationale for Phages as Complements of
708 Antibiotics. Trends Microbiol. 2016;24: 249–256. doi:10.1016/j.tim.2015.12.011

709 54. Arias-Sánchez FI, Allen RC, Hall AR. Effects of prior exposure to antibiotics on bacterial
710 adaptation to phages. J Evol Biol. 2018;11: 2970–10. doi:10.1111/jeb.13220

711 55. Anderl JN, Franklin MJ, Stewart PS. Role of antibiotic penetration limitation in Klebsiella
712 pneumoniae biofilm resistance to ampicillin and ciprofloxacin. Antimicrob Agents
713 Chemother. 2000;44: 1818–1824.

714 56. Pratama AA, van Elsas JD. The “Neglected” Soil Virome – Potential Role and Impact.
715 Trends Microbiol. 2018;: 1–14. doi:10.1016/j.tim.2017.12.004

716

Fig 1

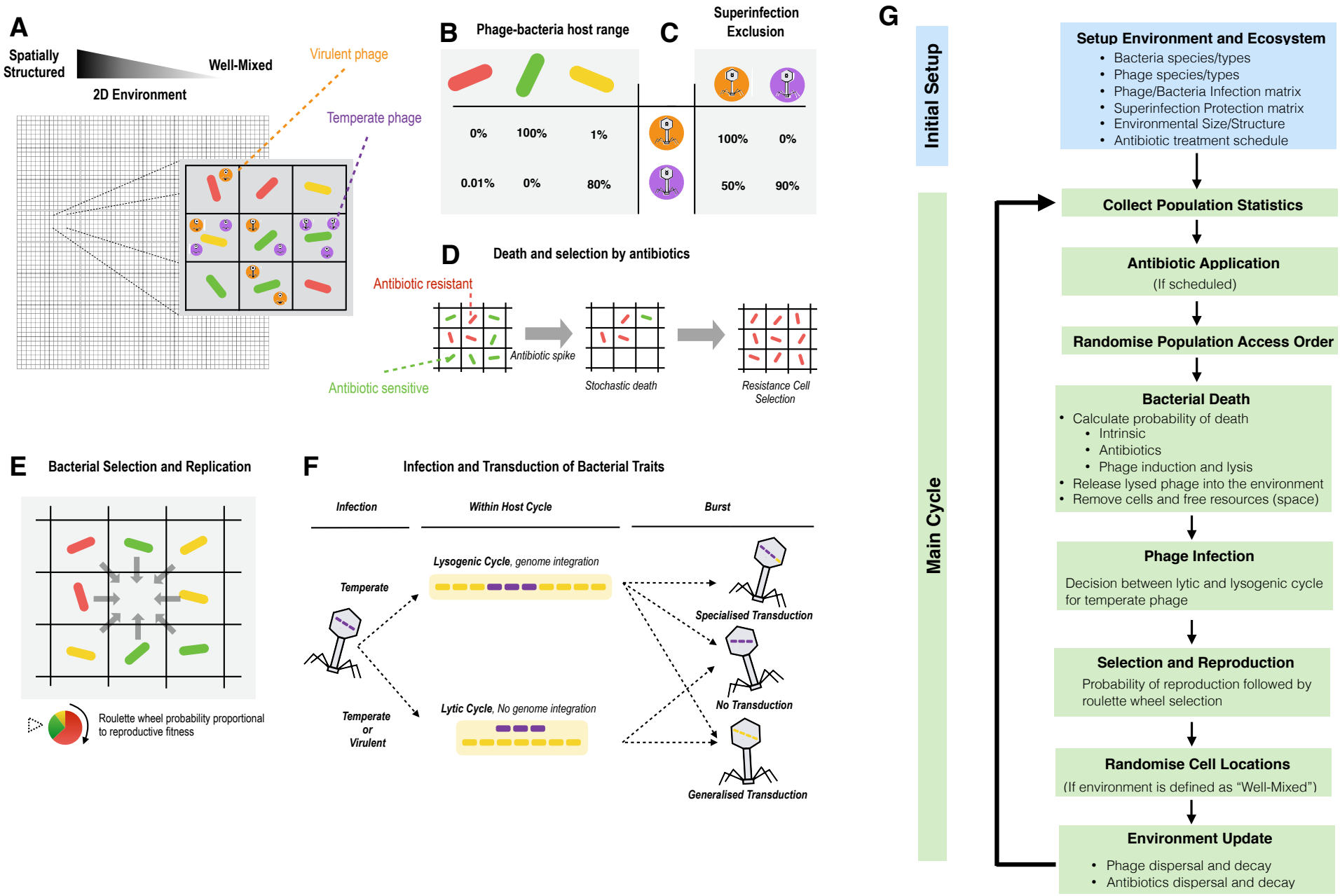
A
Spatially Structured
Well-Mixed
2D Environment
Virulent phage
Temperate phage
B
Phage-bacteria host range
0%
100%
1%
0.01%
0%
80%
C
Superinfection Exclusion
100%
0%
50%
90%
D
Death and selection by antibiotics
Antibiotic resistant
Antibiotic sensitive
Antibiotic spike
Stochastic death
Resistance Cell Selection
E
Bacterial Selection and Replication
Roulette wheel probability proportional to reproductive fitness
F
Infection and Transduction of Bacterial Traits
Infection
Within Host Cycle
Burst
Lysogenic Cycle, genome integration
Temperate
Specialised Transduction
No Transduction
Lytic Cycle, No genome integration
Temperate or Virulent
Generalised Transduction
G
Initial Setup
Setup Environment and Ecosystem
• Bacteria species/types
• Phage species/types
• Phage/Bacteria Infection matrix
• Superinfection Protection matrix
• Environmental Size/Structure
• Antibiotic treatment schedule
Main Cycle
Collect Population Statistics
Antibiotic Application
(If scheduled)
Randomise Population Access Order
Bacterial Death
• Calculate probability of death
• Intrinsic
• Antibiotics
• Phage induction and lysis
• Release lysed phage into the environment
• Remove cells and free resources (space)
Phage Infection
Decision between lytic and lysogenic cycle for temperate phage
Selection and Reproduction
Probability of reproduction followed by roulette wheel selection
Randomise Cell Locations
(If environment is defined as "Well-Mixed")
Environment Update
• Phage dispersal and decay
• Antibiotics dispersal and decay

Fig 2

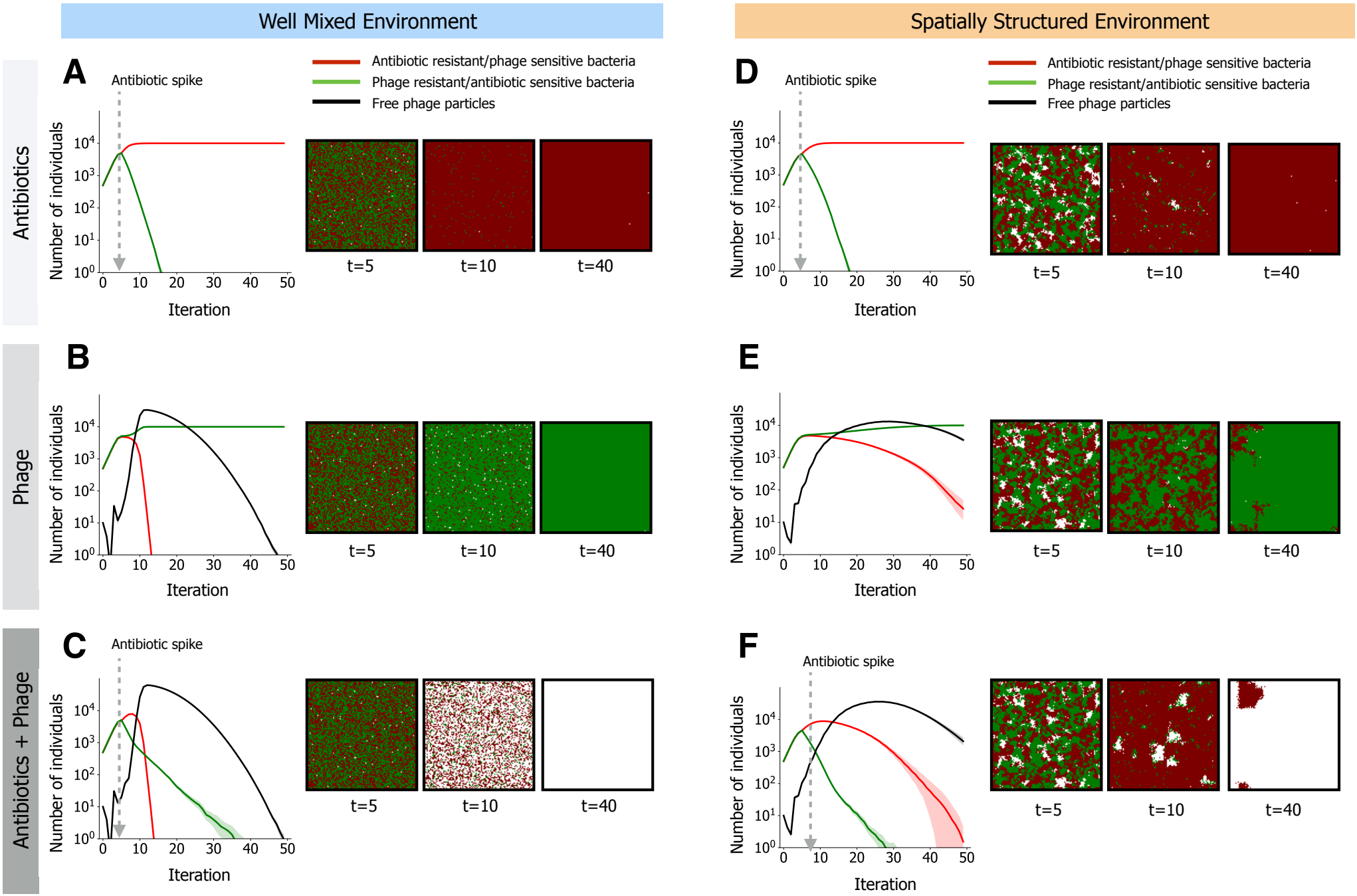
Well Mixed Environment
Spatially Structured Environment
Antibiotics
Phage
Antibiotics + Phage
A
B
C
D
E
F
Antibiotic spike
Antibiotic resistant/phage sensitive bacteria
Phage resistant/antibiotic sensitive bacteria
Free phage particles
Number of individuals
Iteration
t=5
t=10
t=40

Fig 3

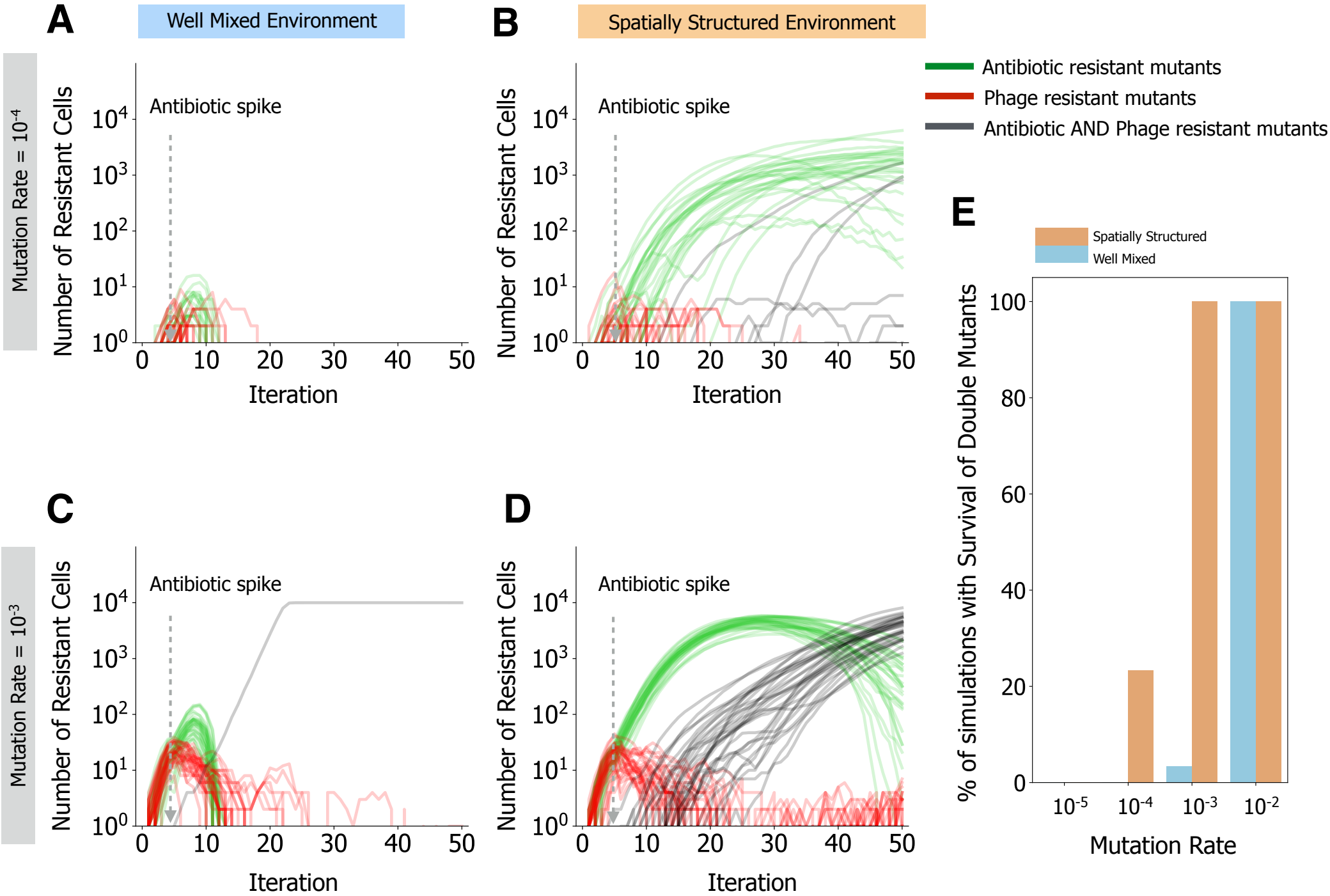
A
Well Mixed Environment
B
Spatially Structured Environment
Antibiotic resistant mutants
Phage resistant mutants
Antibiotic AND Phage resistant mutants
Mutation Rate = 10^{-4}
Mutation Rate = 10^{-3}
Number of Resistant Cells
Antibiotic spike
Iteration
C
D
E
Spatially Structured
Well Mixed
% of simulations with Survival of Double Mutants
Mutation Rate

Fig 4

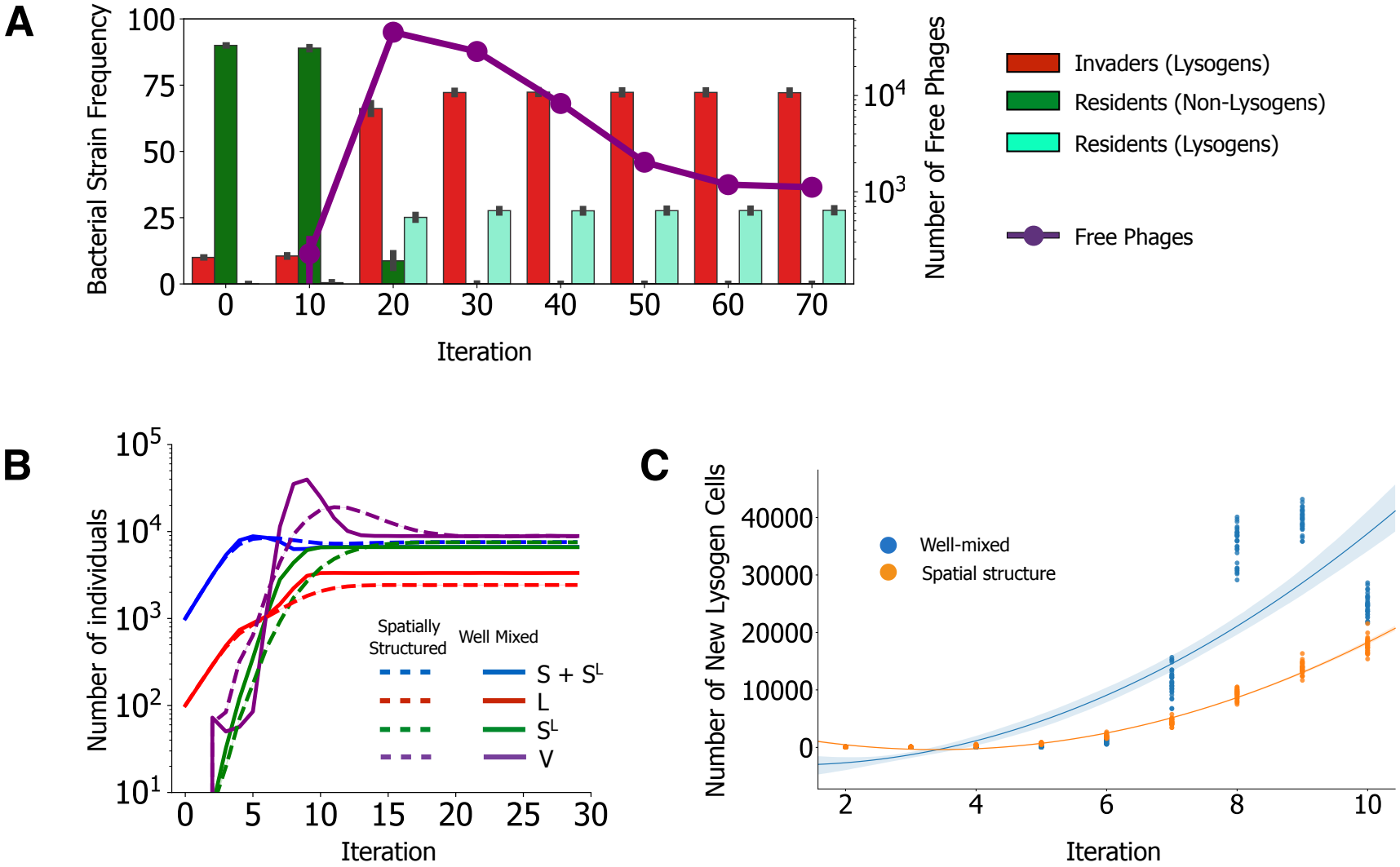
A
Bacterial Strain Frequency
100
75
50
25
0
0
10
20
30
40
50
60
70
Iteration
10^4
10^3
Number of Free Phages
Invaders (Lysogens)
Residents (Non-Lysogens)
Residents (Lysogens)
Free Phages
B
Number of individuals
10^5
10^4
10^3
10^2
10^1
0
5
10
15
20
25
30
Iteration
Spatially Structured
Well Mixed
S + S^L
L
S^L
V
C
Number of New Lysogen Cells
40000
30000
20000
10000
0
2
4
6
8
10
Iteration
Well-mixed
Spatial structure

Fig 5

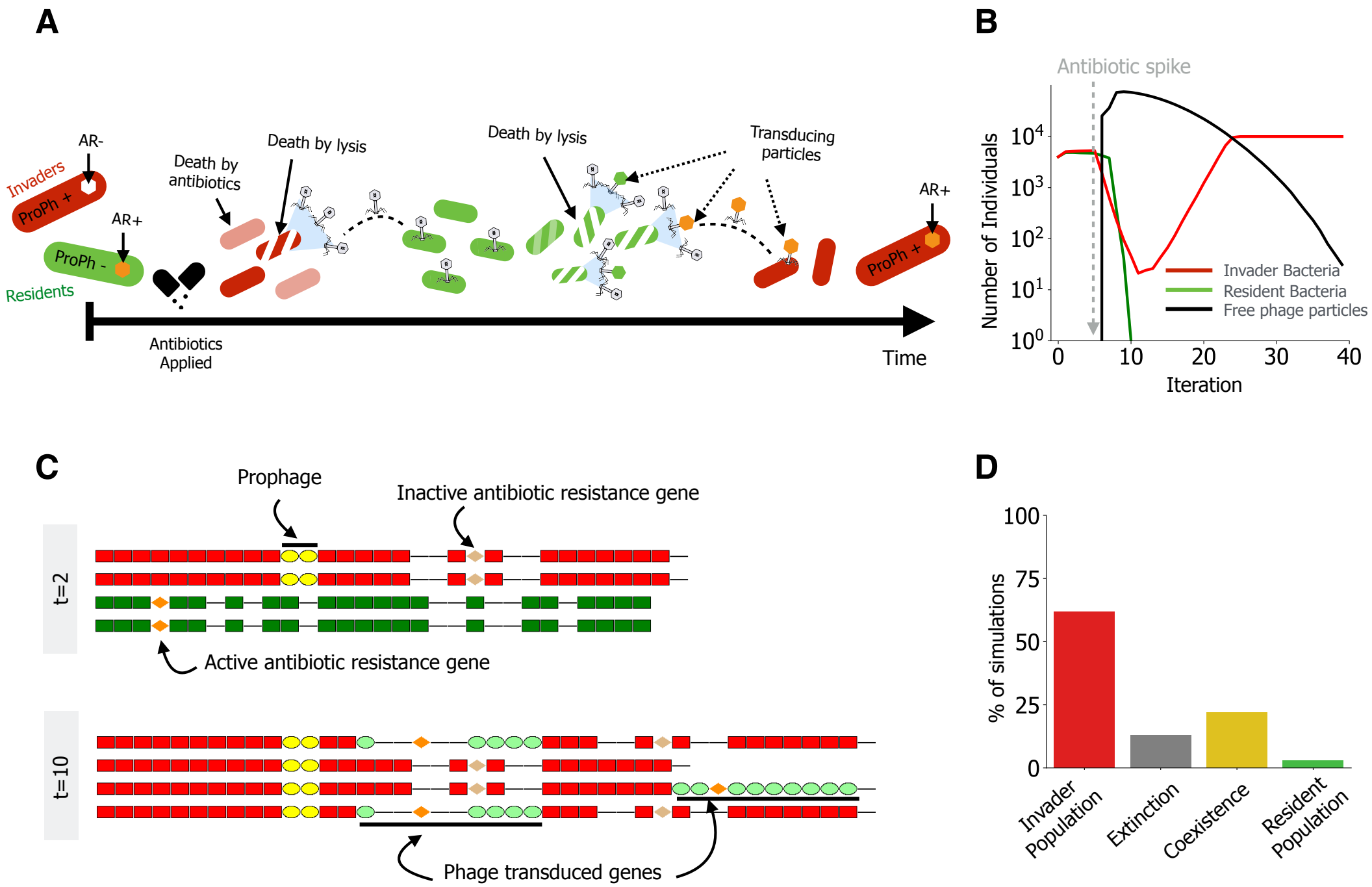
A
AR-
Invaders
ProPh +
AR+
ProPh -
Residents
Death by antibiotics
Death by lysis
Death by lysis
Transducing particles
AR+
ProPh +
Antibiotics Applied
Time
B
Antibiotic spike
Number of Individuals
10^4
10^3
10^2
10^1
10^0
0
10
20
30
40
Iteration
Invader Bacteria
Resident Bacteria
Free phage particles
C
Prophage
Inactive antibiotic resistance gene
t=2
Active antibiotic resistance gene
t=10
Phage transduced genes
D
% of simulations
100
75
50
25
0
Invader Population
Extinction
Coexistence
Resident Population

Fig 6

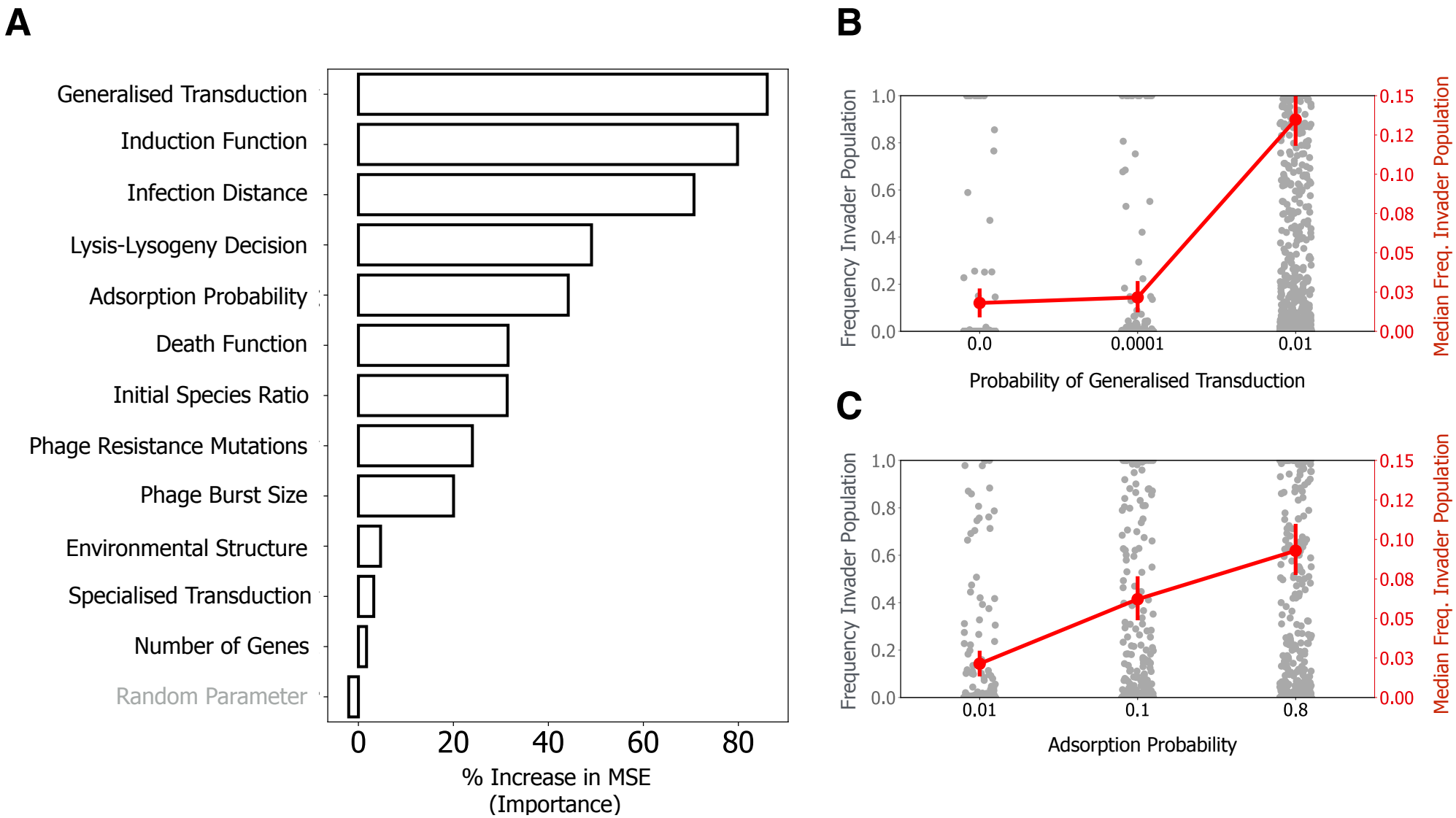
A
Generalised Transduction
Induction Function
Infection Distance
Lysis-Lysogeny Decision
Adsorption Probability
Death Function
Initial Species Ratio
Phage Resistance Mutations
Phage Burst Size
Environmental Structure
Specialised Transduction
Number of Genes
Random Parameter
0
20
40
60
80
% Increase in MSE
(Importance)
B
Frequency Invader Population
Median Freq. Invader Population
1.0
0.8
0.6
0.4
0.2
0.0
0.15
0.12
0.10
0.08
0.05
0.03
0.00
0.0
0.0001
0.01
Probability of Generalised Transduction
C
Frequency Invader Population
Median Freq. Invader Population
1.0
0.8
0.6
0.4
0.2
0.0
0.15
0.12
0.10
0.08
0.05
0.03
0.00
0.01
0.1
0.8
Adsorption Probability

Fig 7

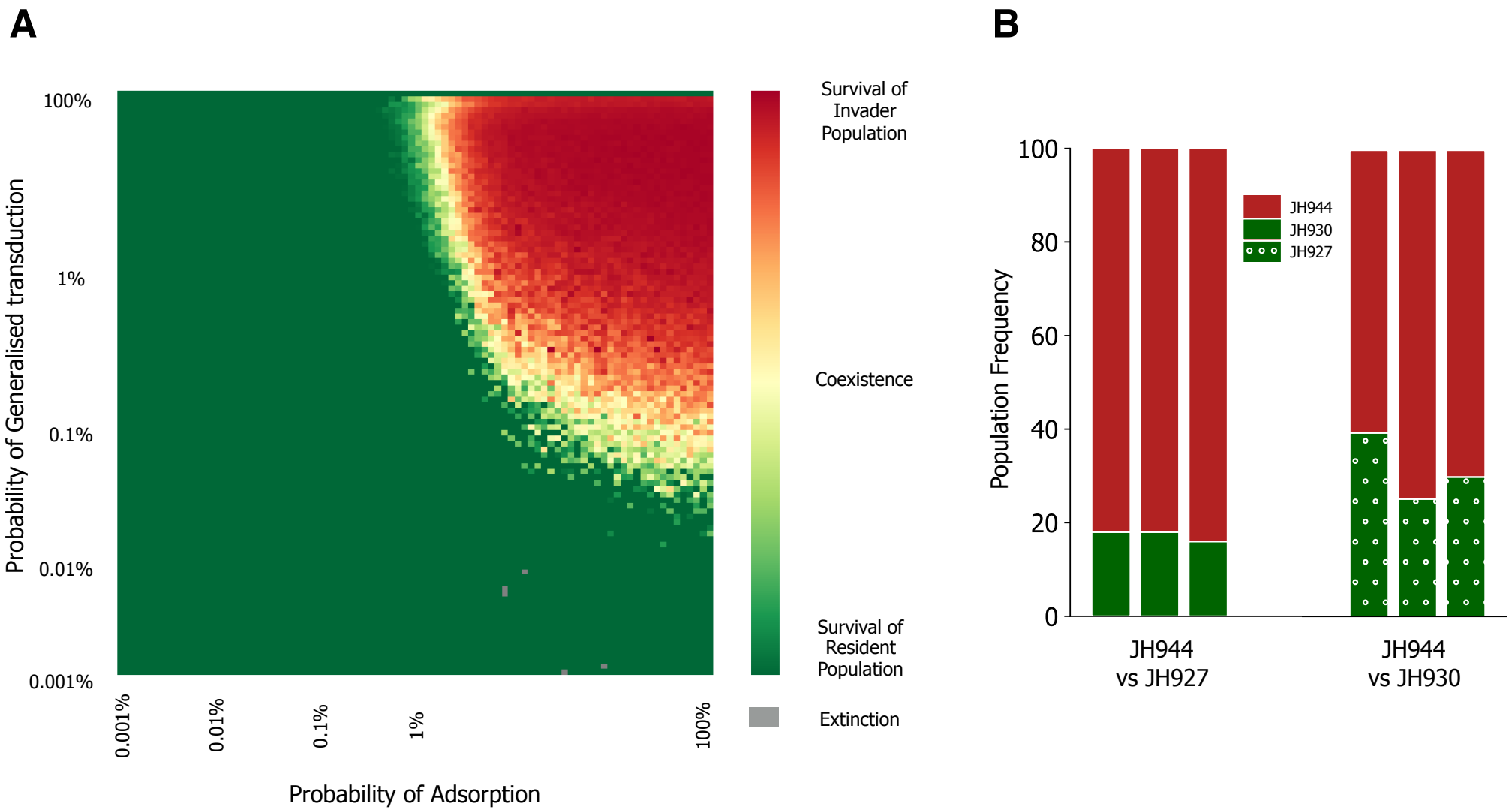
A
100%
1%
0.1%
0.01%
0.001%
Probability of Generalised transduction
0.001%
0.01%
0.1%
1%
100%
Probability of Adsorption
Survival of Invader Population
Coexistence
Survival of Resident Population
Extinction
B
100
80
60
40
20
0
Population Frequency
JH944
JH930
JH927
JH944 vs JH927
JH944 vs JH930